Does density-functional theory predict a spin-density-wave ground state for Cr?

2001 J. Phys.: Condens. Matter 13 L239

(http://iopscience.iop.org/0953-8984/13/11/104)

INSTITUTE OF PHYSICS PUBLISHING JOURNAL OF PHYSICS: CONDENSED MATTER

J. Phys.: Condens. Matter **13** (2001) L239–L247 www.iop.org/Journals/cm PII: S0953-8984(01)22062-1

LETTER TO THE EDITOR

Does density-functional theory predict a spin-density-wave ground state for Cr?

R Hafner, D Spišák, R Lorenz and J Hafner

Institut für Materialphysik and Centre for Computational Material Science, Universität Wien, Sensengasse 8, A-1090 Wien, Austria

Received 16 February 2001

Abstract

We present *ab initio* spin-density-functional investigations of static long-period spin-density waves (SDWs) in Cr. Calculations performed in the generalized-gradient approximation (GGA) and using both projector-augmented-wave and muffin-tin orbital techniques show that the overestimation of the strength of the antiferromagnetism suppresses the formation of an SDW. In the local density approximation we find that a static SDW is also higher in energy than a commensurate antiferromagnetic structure, but with an energy difference that tends towards zero as the lattice constant shrinks to its low-temperature limit. A possible scenario for the origin of the observed SDW state is developed.

The incommensurate spin-density-wave magnetism of Cr has attracted great interest since its discovery via neutron scattering [1, 2]. At low temperature, Cr exhibits a linearly polarized incommensurate spin-density wave (SDW), which consists of a roughly sinusoidal modulation of the magnetic moments:

$$\vec{m}(\vec{R}) = \vec{m}_0 \sin(\vec{q} \cdot \vec{R})$$

with an amplitude of $m_0 \sim 0.5\ \mu_B$ and an incommensurate wavevector of

$$\vec{q} = 2\pi a(1-\delta)\vec{e}_x = \vec{G}_{100}(1-\delta).$$

δ measures the deviation from a commensurate antiferromagnetic structure. The periodicity of the SDW is given by $\lambda = a/\delta$ and, since $\delta \sim 0.05$, the wavelength of the SDW is about 60 Å (or 42 interlayer distances) in the low-temperature limit, increasing to about 78 Å at room temperature. At low T, the SDW is longitudinal ($\vec{q} \parallel \vec{m}$), but at $T_s \simeq 123$ K a spin-flip transition to a transverse SDW ($\vec{q} \perp \vec{m}$) occurs. Above the Néel temperature of $T_N = 311$ K, Cr is paramagnetic (for more details, we refer the reader to the reviews of Fawcett [3] and Zabel [4]. The incommensurate SDW structure of Cr is very sensitive to elastic strain or changes of the valence electron concentration, which may stabilize a commensurate antiferromagnetic (AFM1) structure with a higher magnetic moment and Néel temperature. Just 0.3 at.% Mn in Cr is sufficient to stabilize an AFM1 configuration with $m_0 \simeq 0.8\ \mu_B$ and $T_N = 600$ K [5, 6].

The first explanation of the occurrence of an incommensurate SDW in Cr was given by Overhauser [7]. He argued that the pronounced nesting properties of the Fermi surface of

paramagnetic Cr lead to an instability against the formation of a spin-density wave. The nesting vector $\vec{q}$ connecting electron and hole surfaces couples eigenstates of electrons and holes in such way that occupied states are lowered and unoccupied states are raised in energy. The nesting vector is incommensurate because the hole Fermi surface is slightly larger than the electron Fermi surface. At finite temperature, electrons are excited across the gaps creating by the nesting, causing further reduction of the SDW amplitude. The nesting properties of the experimental Fermi surface [8] have been confirmed in detail by density-functional calculations [9–11], but attempts to determine the magnetic ground state have been restricted to the commensurate antiferromagnetic (AFM1) state.

However, even spin-density-functional investigations of paramagnetic and commensurate antiferromagnetic Cr are not entirely unproblematic, as evidenced by the large scatter of the results reported in the literature [9–17]. Calculations performed in the local spin-density approximation (LSDA) agree qualitatively on the fact that at the equilibrium density, Cr is nonmagnetic or marginally antiferromagnetic, but disagree substantially on the magnetic moment at equilibrium. For example Kübler [10, 11] used the augmented-spherical-wave (ASW) method and predicted an equilibrium lattice constant of $a = 2.854$ Å (experiment: $a = 2.884$ Å) and a magnetic moment of $m = 0.59\ \mu_B$ at equilibrium and of $m = 0.71\ \mu_B$ at the experimental density. Marcus *et al* [16], also using the ASW method and the LSDA, found $a = 2.842$ Å and a nonmagnetic ground state; at equilibrium density their calculated moment compares very well with Kübler's value. Chen, Singh and Krakauer [13] reported $a = 2.798$ Å, a nonmagnetic ground state and $m = 0.70\ \mu_B$ at the equilibrium lattice constant. Singh and Ashkenazi [15] used the full-potential augmented-plane-wave (FLAPW) method to investigate the influence of nonlocal corrections to the exchange–correlation functional in the form of a generalized-gradient approximation (GGA). With the GGA proposed by Perdew and Wang [18], they found a lattice constant of $a = 2.91$ Å (i.e. larger than that from experiment) for an antiferromagnetic ground state with $m = 1.55\ \mu_B$ and $m = 1.4\ \mu_B$ at the experimental density. The huge increase in the stability of the antiferromagnetic state and of the magnetic moment is not confirmed by the recent FLAPW calculations of Blügel and co-workers [17] who found using the GGA $a = 2.85$ Å and $m = 0.99\ \mu_B$, the calculated LSDA lattice constant being, at $a = 2.79$ Å, considerably smaller than the previous ASW predictions, but in agreement with the earlier FLAPW results. The use of the gradient corrections improves not only the prediction of the lattice parameter, but also leads to a much better bulk modulus; the tendency to overestimate the magnetic moment, however, is obvious. This comparison underlines the difficulty, already emphasized by Marcus *et al* [16], of accurately assessing the ground-state properties of Cr. The comparison the LSDA and GGA for Cr is in contrast to the results for other ferromagnetic (Fe) [19] and antiferromagnetic (Mn) [20] 3d metals where the GGA not only improves the calculated mechanical properties, but is also essential for a correct prediction of the magnetic ground state.

Only recently have attempts been made to apply density-functional theory (DFT) to the incommensurate SDW state of Cr. Hirai [21] used the LSDA and the Korringa–Kohn–Rostoker (KKR) Green's-function method to calculate the total energy of a few commensurate SDW states with wavevectors close to the experimental incommensurate wavevector $\vec{q} = a^*(0.952, 0, 0)$, with $a^* = 2\pi/a$. At a density corresponding to the experimental lattice constant, the total energy of a SDW with $q = a^*(19/20, 0, 0)$ was found to be lower by about $\Delta E \sim 0.01$ to 0.02 mRyd/atom than that for states with slightly different periodicities ($q/a^* = 17/18$ and $q/a^* = 21/22$; the energy difference is reported only in a graph). No energy difference between the SDW and the AFM1 states is reported in the published paper, but according to Hirai [22] the energy differences are ΔE(SDW–AFM1) $= 0.011$ mRyd and ΔE(AFM1–NM) $= 0.097$ mRyd/atom. One should note that the energy difference

between the antiferromagnetic and the paramagnetic states corresponds to a temperature of only $T \sim 15$ K—this is hardly compatible with the observed Néel temperature. Very recently, Blügel and co-workers [17] applied the FLAPW method within the GGA to the same problem. However, since the FLAPW technique does not allow one to handle systems with a periodicity that is as large as that found experimentally for the SDW state of Cr, only two commensurate SDWs with $q/a^* = 11/12$ and $13/14$ were calculated. The energy difference with respect to the AFM1 state was found to be $\Delta E = 0.71$ mRyd/atom for $q/a^* = 12/13$ and $\Delta E = -0.35$ mRyd/atom for $q/a^* = 13/14$. Note that the energy difference between these two SDW states and the AFM1 state is more than an order of magnitude larger than Hirai's energy difference of 0.011 mRyd/atom between the $q/a^* = 19/20$ SDW and the commensurate antiferromagnetic state. On the basis of a rather daring interpolation between these wavevectors and $q/a^* = 1$ (the AFM1 state) it was concluded that the true energy minimum occurs close to the experimentally observed SDW wavevector. The problematic point with this result is that the large change in energy on going from $q/a^* = 12/13$ to $13/14$ would mean that there is already a relatively large energy gain when the nesting is still far from perfect. This is hard to reconcile with the well-known sensitivity of the SDW state to even small changes in the Fermi energy (alloying of just 0.3 at.% Mn is sufficient to stabilize a commensurate AFM1 state [3]).

The aim of the present work was to perform a thorough analysis of the energetics of SDW formation in Cr within DFT, using both the LSDA and the GGA and covering the entire range of wavevectors of interest. This task goes to the very limits of the capability of even the most advanced electronic structure codes, both because of the long wavelength of the SDW and because of the smallness of the energy differences involved. In order to consolidate our results, we used two different techniques: the projector-augmented-wave (PAW) method, [23] as implemented in the Vienna *ab initio* simulation package (VASP) [24] and the linearized muffin-tin orbital (LMTO) method in the atomic sphere approximation (ASA) [25]. The PAW method is an extremely accurate, yet highly efficient all-electron full-potential technique based on a plane-wave expansion of the electronic eigenstates. The LMTO-ASA uses a simplified geometry of the effective one-electron potential and a minimal s, p, d basis set. In all calculations we used the LDA exchange–correlation functional of Perdew and Zunger [26], eventually supplemented with the generalized-gradient corrections proposed by Perdew *et al* [27] and using the spin interpolation of Vosko, Wilk and Nusair (VWN) [28] for all spin-polarized calculations. To achieve the accuracy necessary to obtain reliable energy differences, it is very important to achieve full convergence of the Brillouin-zone integrations. We used fine Monkhorst–Pack [29] grids with 28 special $\boldsymbol{k}$-points within the irreducible Brillouin zone for a cell containing 28 Cr atoms used for modelling a commensurate SDW with $q/a^* = 13/14$—this is the same set-up as is used in the FLAPW calculations of Blügel and co-workers [17]—in combination with Methfessel–Paxton smearing [30]. A corresponding set-up has been used for all other calculations.

We begin with a brief look at the properties of bulk bcc Cr as described in the LSDA and the GGA. The calculated lattice constants, bulk moduli and magnetic moments at equilibrium and at the experimental density are summarized in table 1; figure 1 displays the variation of the magnetic moment as a function of the lattice constant. The lattice constant calculated in the GGA is about 1% smaller than that found in the experiment; the bulk modulus shows excellent agreement. Our PAW results are almost identical with the FLAPW result of Blügel and co-workers [17], but in disagreement with earlier the FLAPW–GGA results discussed above. It is evident that at equilibrium the LSDA underestimates and the GGA overestimates the magnetic moment of Cr and that the moments show a strong dependence on the lattice constant (see figure 1). While the GGA predictions for the lattice constant and bulk modulus are

Table 1. The lattice constant, cohesive energy, bulk modulus and magnetic moment of bcc Cr in the paramagnetic and antiferromagnetic states.

		a (Å)	E_{coh} (eV)	B (Mbar)	m (μ_B)[a]	m (μ_B)[b]
LSDA	PM	2.779	5.083	3.03	—	—
	AFM	2.778	5.681	2.92	0.00	0.67
GGA	PM	2.836	4.147	2.61	—	—
	AFM	2.849	4.154	1.89	0.92	1.19
Experiment[c]	AFM	2.884	4.095	1.90	0.60	0.60

[a] The magnetic moment at the theoretical equilibrium lattice constant.
[b] The magnetic moment at the measured lattice constant.
[c] Reference [3].

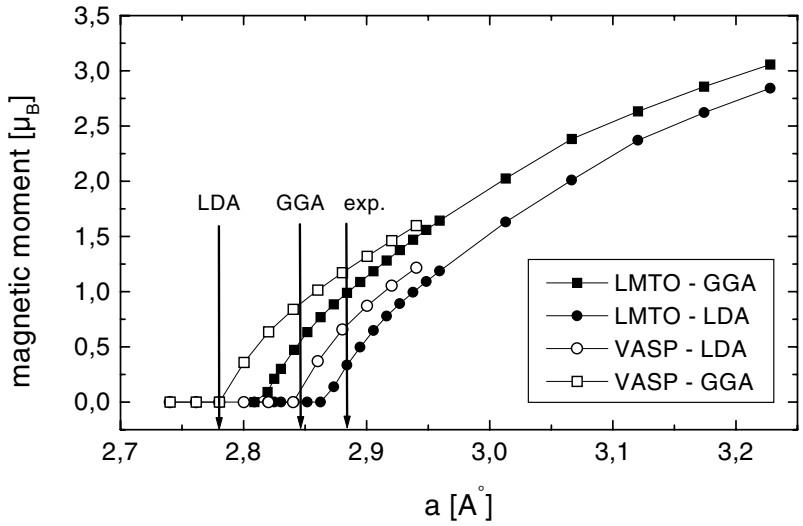

Figure 1. The magnetic moment of commensurate antiferromagnetic Cr as a function of the lattice constant, as calculated using the LMTO (full symbols) and VASP–PAW (open symbols) methods plus the LSDA (circles) and the GGA (squares). Vertical arrows indicate the equilibrium and the experimental lattice constants (cf. table 1).

definitely superior to the LSDA values, we have to note that the GGA moment is about twice as large as the experimentally determined amplitude of the SDW. Close to the breakdown of antiferromagnetism, the full-potential PAW calculations tend to predict larger magnetic moments than the LMTO calculations using the atomic sphere approximation—evidently this is due to the spherical averaging over spin densities and exchange potentials. At lower densities where the antiferromagnetism is stabilized, this difference gradually vanishes. Figure 2 shows the Fermi surfaces of paramagnetic and antiferromagnetic Cr, calculated using the GGA. The nesting vector associated with SDW formation is $\vec{q}_1$; its length is calculated to be $q_1/a^* = 0.952$, in excellent agreement with the experimental Fermi surface. Both the Fermi surface and the nesting vectors are almost identical in the GGA and LSDA; hence the nesting mechanism is not affected by the choice of the exchange–correlation functional.

Figure 3 shows the difference in total energy between the SDW and AFM1 states as a function of the wavevector $\vec{q}$, as calculated using the VASP–PAW and LMTO-ASA methods and using the experimental lattice constant in both cases. In the LMTO-ASA the calculations

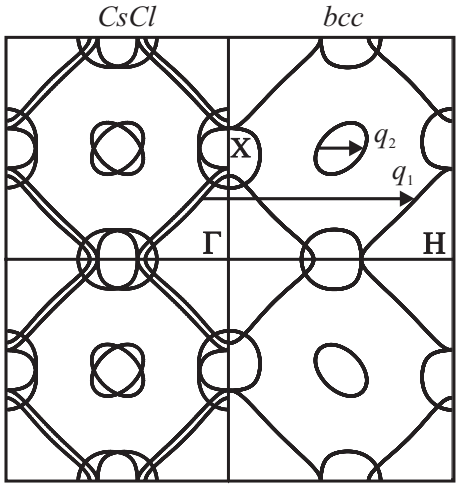

Figure 2. Fermi surface contours of paramagnetic Cr in the (001) plane (right panel); the left panel shows the same contours downfolded to the Brillouin zone of the commensurate antiferromagnetic structure. GGA calculations using the LMTO-ASA. The calculated magnitude of the nesting vector $\vec{q}_1$ shown in the graph is $q_1/a^* = 0.952$.

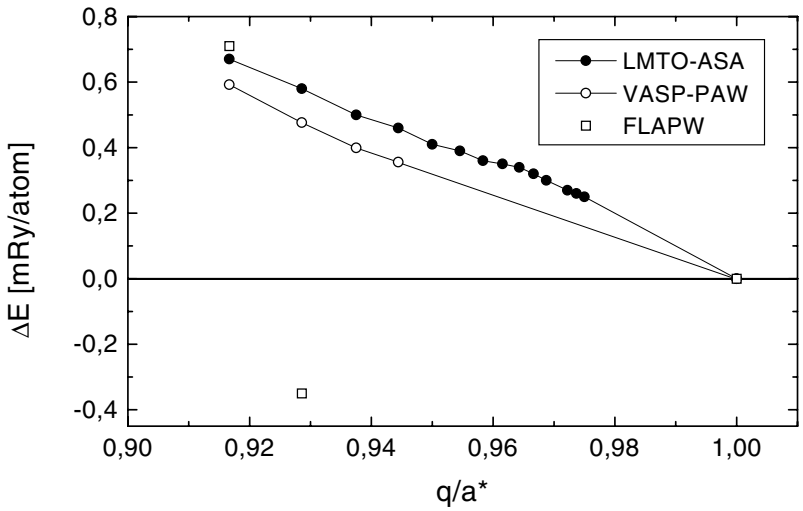

Figure 3. The variation of the energy difference between the SDW and the commensurate AFM1 state of Cr as a function of the wavevector. Full dots: LMTO-ASA results; empty circles: VASP–PAW results; squares: FLAPW results of reference [17]. All calculations use the GGA.

have been extended to $q/a^* = 39/40$, i.e. to very elongated tetragonal cells with one atom in the (100) plane but containing altogether 80 atoms. Both methods predict an almost linear dependence of the energy difference on the wavevector of the SDW—the close agreement between the results obtained with two radically different techniques should be noted. For $q/a^* = 11/12$ the VASP–PAW result is in excellent agreement with the FLAPW result of Blügel and co-workers [17], but we are unable to reproduce their negative energy difference for $q/a^* = 13/14$. Our result means that the GGA fails to produce a stable SDW for Cr. The almost linear dependence of the energy difference on the wavevector indicates that the energy

loss disfavouring the SDW state arises from the necessity to quench the magnetic moments in the vicinity of the node in the SDW. As the moments calculated in the GGA are too large, this energy loss is too large to be overcompensated by a gain in nesting energy. The extension of the region in which the moments are quenched varies only little with $\vec{q}$—this explains the linear variation of the energy difference with the length of the supercell. The profile of the SDW is not exactly sinusoidal, but—especially for very long wavelengths—more rectangular, corresponding to a $\sin(3\vec{q}\cdot\vec{R})$ overtone out of phase with the basic $\sin(\vec{q}\cdot\vec{R})$ SDW, in agreement with experiment [3]. Details will be reported elsewhere.

Figure 4 analyses the variation of the amplitude of the magnetic moment as a function of q. We find that the creation of a SDW reduces the magnetic moment, but at the experimental value of $q/a^* \simeq 0.952$, the calculated moments are still larger ($m_0 \geqslant 0.8\,\mu_B$) than the experimentally determined amplitude of the SDW. At smaller wavevectors the magnetic moments calculated using the LMTO decrease very rapidly, because the frustration becomes too strong. In the PAW and FLAPW calculations, larger moments persist at smaller q, although the energy differences relative to the AFM1 state are almost the same in the PAW and LMTO methods. The difference between the PAW/FLAPW and LMTO calculations is clearly related to the use of the ASA for potentials and charge densities in the LMTO. The spherical averaging in overlapping atomic spheres has a tendency to smooth gradients in the exchange potential and spin densities.

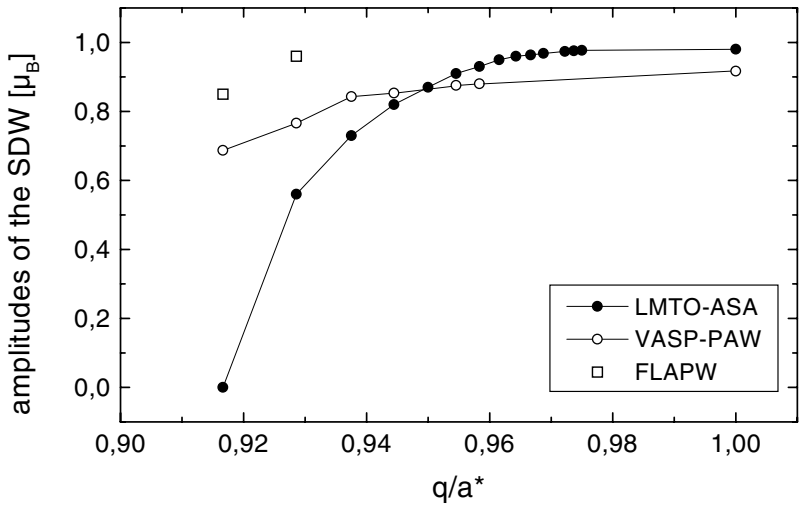

Figure 4. The variation of the amplitude m_0 of the SDW as a function of the wavevector q as calculated in the GGA. Full dots: LMTO-ASA results; empty circles: VASP–PAW results; squares: FLAPW results (reference [17]).

The instability of SDWs result suggests seeking for an SDW solution in the LSDA, which produces significantly lower magnetic moments around the equilibrium density. As the magnetic moment calculated in the LSDA shows almost critical behaviour in this range, we performed the LSDA calculations at different lattice constants. At the experimental lattice constant of $a = 2.884$ Å where the LMTO moment is found to be only $m = 0.33\ \mu_B$, magnetism disappears at $q/a^* \leqslant 0.97$, and therefore an SDW solution with the experimental wavevector is unstable. Hence we have to look for a possible SDW solution at slightly larger lattice parameters where the AF moment is larger. Figure 5 shows the variation of the total energy, figure 6 that of the amplitude of the SDW with the wavevector, for lattice constants that are between 0.4% and 0.8% larger than the experimental value. Although

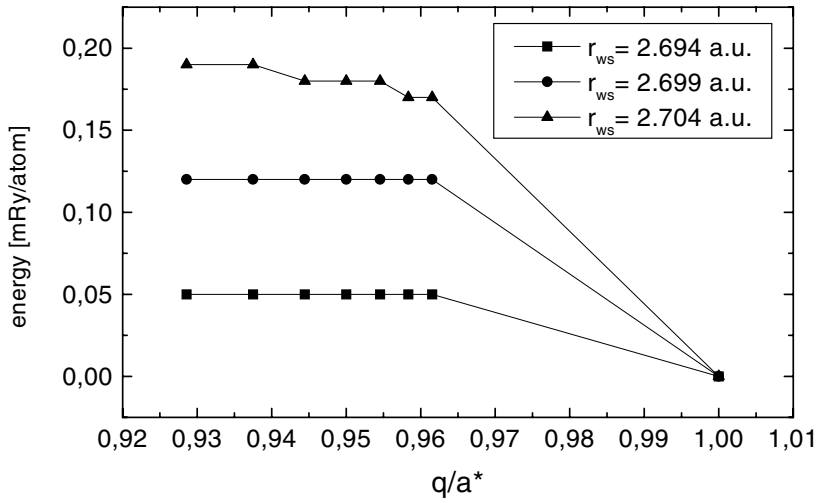

Figure 5. The variation of the energy difference between the SDW and the commensurate AFM1 state of Cr as a function of the wavevector q as calculated in the LSDA with the LMTO-ASA. Squares: $a = 2.895$ Å; circles: $a = 2.900$ Å; triangles: $a = 2.906$ Å.

the energy difference ΔE(SDW–AFM1) is strongly reduced compared to the GGA solution, the qualitative result remains the same: no minimum representing a stable SDW state could be detected. At the lattice constant of $a = 2.895$ Å with an AFM1 moment of 0.50 μ_B, magnetism disappears at $q/a^* \leqslant 0.95$. A further expansion of the bcc lattice by $\leqslant 0.4\%$ stabilizes the magnetic order, but even at $a = 2.906$ Å the magnetic moments break down at SDW wavevectors that are only slightly smaller than the experimental value. Parallel to the increasing magnetic moment, the energy difference between the incommensurate SDW and the AFM1 states increases from ΔE(SDW–AFM1) $\leqslant 0.01$ mRyd/atom at $a = 2.884$ Å to ΔE(SDW–AFM1) $\simeq 0.17$ mRyd/atom at $a = 2.906$ Å (both referring to $q/a^* = 0.952$). The reason is again that with increasing amplitude the energy loss from the frustration in the regions of the node increases. The important message is that in no case is the nesting energy sufficient to stabilize a SDW with a periodicity in the range between 30 and 60 interlayer distances. The GGA calculations have not been repeated at different volumes, but it is not to be expected that this would lead to a different scenario, given the similarity of the LSDA and GGA Fermi surfaces. Our results agree with those of Hirai insofar as with the LSDA, the energy difference ΔE(SDW–AFM1) is smaller than a few hundreds of a mRyd—in our opinion this means that it is at the margin or even below computational accuracy. There is an important difference in the magnitude of the magnetic moments: Hirai's AFM1 moment of $m = 0.7\ \mu_B$ is significantly larger than ours (and also than recent FLAPW calculations in the LSDA) and persists down to rather small values of q. It is difficult to understand how these relatively large moments are compatible with such minimal energy differences—this concerns not only the SDW state, but also (and more importantly) the difference between the NM and AFM1 states.

It is known that the SDW is coupled to a strain wave [4]. VASP allows for a calculation of the Hellmann–Feynman forces acting on the atoms and for a structural relaxation of the SDW. In the PAW calculations for SDW states at fixed interplanar distances, the calculated forces on the atoms do indeed indicate a tendency to shrink the distances around the nodes of the SDW. However, as expected from the very small magnetovolume effect in Cr (see table 1), and in

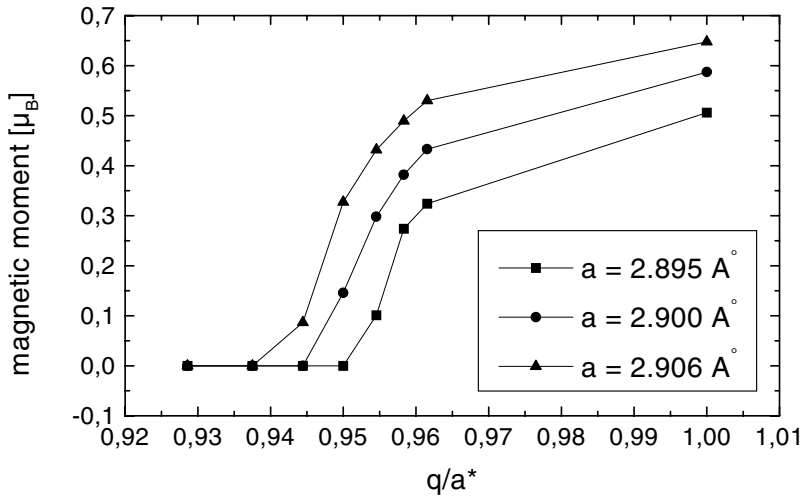

Figure 6. The variation of the amplitude μ_0 of the SDW as a function of the wavevector q as calculated in the LSDA with the LMTO-ASA. Squares: $a = 2.895$ Å; circles: $a = 2.900$ Å; triangles: $a = 2.906$ Å.

agreement with the very small amplitude ($A \sim 3.5 \times 10^{-3}a$) of the strain wave deduced from the neutron scattering data, the SDW-induced stresses are too weak to allow for an efficient multiparameter optimization of the SDW supercell calculations. An SDW–GGA calculation with relaxed interplanar distances leads to the conclusion that these relaxations are too weak to be determined quantitatively at the level of accuracy of our present calculations. The important conclusion, however, is that the stress relaxation has no significant effect on the energetics of the SDW phase.

Hence we are led to the following conclusions:

(i) The overestimation of the magnetic moments in the GGA suppresses the formation of a stable SDW in Cr. The energy necessary to quench the magnetic moments in the vicinity of the nodes in the SDW is too high to be overcompensated by the gain in the nesting energy.

(ii) In the LSDA, Cr is only weakly magnetic at the experimental density. Under these conditions, the energy difference between the AFM1 and SDW states is essentially zero at the level of accuracy of our calculations ($\Delta E \leqslant 0.01$ mRyd/atom corresponding to a temperature of 1.6 K). The amplitude of the SDW is only $\sim$0.1 μ_B at the experimental wavevector.

(iii) Even a very modest expansion of the lattice constant leads to a significant increase of the magnetic moment and of the SDW–AFM1 energy difference, an expansion of $\sim$0.5% leads to an amplitude of the SDW of $m_0 = 0.3$ μ_B and an energy difference of ΔE(SDW–AFM1) $\sim$ 0.12 mRyd/atom.

(iv) Although DFT calculations do not predict an SDW ground state, the excitation energies for creating a SDW are within the range of thermal energies even well below the Néel temperature. In addition, our calculations show that the contraction of the lattice on cooling leads to a reduction of the excitation energy—hence SDWs excited at higher temperature will not be frozen out as the temperature is lowered. SDWs with the 'nesting' wavevector are favoured, because of the larger number of low-energy excitations.

(v) These conclusions are unlikely to be modified qualitatively by the choice of a different exchange–correlation functional. Any gradient correction will show a tendency to overestimate the strength of the antiferromagnetism. However, the LSDA seriously underestimates the equilibrium density. The situation that we have found for Cr contrasts with that established for Mn and Fe, where the GGA is necessary for an even qualitatively correct assessment of the magnetic ground state [19, 20].

(vi) In the main, we tend to agree with the analysis of Marcus *et al* [16] relating the properties of SDW Cr to the small energy differences between NM and AFM1 Cr and to their extreme sensitivity to volume, combined with the tendency to form dynamical SDWs favoured by the nesting properties.

In summary, very accurate DFT calculations using two different codes based on plane-wave and muffin-tin orbital basis sets demonstrate that in neither of its variants does DFT predict a stable SDW ground state of Cr. Calculations based on the LSDA suggest a possible scenario of dynamical SDW excitations stabilized at low temperatures by a decreasing excitation energy. The enhanced magnetism resulting from the GGA tends to suppress SDW formation.

This work was supported by the Austrian Science Fund under project No P12783-PHYS.

References

[1] Corliss L, Hastings J M and Weiss R J 1959 *Phys. Rev. Lett.* **3** 211
[2] Bykov V N *et al* 1958 *Dokl. Akad. Nauk SSSR* **4** 1149
[3] Fawcett E 1988 *Rev. Mod. Phys.* **60** 209
[4] Zabel H 1999 *J. Phys.: Condens. Matter* **11** 9303
[5] Fawcett E *et al* 1994 *Rev. Mod. Phys.* **66** 25
[6] Jiang X W and Fishman R S 1997 *J. Phys.: Condens. Matter* **9** 3417
[7] Overhauser A W 1962 *Phys. Rev.* B **128** 1437
[8] Lomer W M 1962 *Proc. Phys. Soc.* **80** 489
[9] Laurent D G *et al* 1981 *Phys. Rev.* B **23** 4977
[10] Kübler J 1980 *J. Magn. Magn. Mater.* **20** 277
[11] Kübler J 2000 *Theory of Itinerant Magnetism* (Oxford: Oxford University Press) p 212 ff
[12] Fry J L, Brener N E, Laurent D G and Callaway J 1981 *J. Appl. Phys.* **52** 2101
[13] Chen J, Singh D and Krakauer H 1988 *Phys. Rev.* B **38** 12 834
[14] Moruzzi V L and Marcus P M 1992 *Phys. Rev.* B **42** 4361
[15] Singh D and Ashkenazi J 1992 *Phys. Rev.* B **46** 11 570
[16] Marcus P M, Qiu S L and Moruzzi V L 1998 *J. Phys.: Condens. Matter* **10** 6541
[17] Bihlmayer G, Asada T and Blügel S 2000 *Phys. Rev.* B **62** 11 937
[18] Perdew J P and Wang Y 1992 *Phys. Rev.* B **45** 13 244
[19] Moroni E G, Kresse G, Furthmüller J and Hafner J 1997 *Phys. Rev.* B **56** 15 629
[20] Eder M, Hafner J and Moroni E G 2000 *Phys. Rev.* B **61** 11 492
[21] Hirai K 1997 *J. Phys. Soc. Japan* **60** 560
[22] Hirai K, private communication
According to Dr Hirai, the calculated total energies in the AFM1, SDW (with $q/a^* = 19/20$) and NM states are $E(\mathrm{AFM1}) = -2084.724\,070$ Ryd, $E(\mathrm{SDW}) = -2084.724\,081$ Ryd, $E(\mathrm{NM}) = -2084.723\,973$ Ryd. We thank Dr K Hirai for communicating these unpublished data.
[23] Blöchl P 1994 *Phys. Rev.* B **50** 17 953
[24] Kresse G and Joubert D 1999 *Phys. Rev.* B **59** 1758
[25] Skriver H L 1984 *The LMTO Method (Springer Series)* (Berlin: Springer)
[26] Perdew J P and Zunger A 1981 *Phys. Rev.* B **23** 5048
[27] Perdew J P, Chevary J A, Vosko S H, Jackson K A, Pedersen M R, Singh D J and Fiolhais C 1992 *Phys. Rev.* B **46** 6671
[28] Vosko S H, Wilk L and Nusair M 1980 *J. Can. Phys.* **58** 1200
[29] Monkhorst H J and Pack J D 1976 *Phys. Rev.* B **13** 5188
[30] Methfessel M and Paxton A 1989 *Phys. Rev.* B **40** 3616